SCIENTIFIC REPORTS

OPEN

SUBJECT AREAS:
NANOPARTICLES
OPTICAL MATERIALS

Received
24 September 2013

Accepted
2 December 2013

Published
13 January 2014

Correspondence and requests for materials should be addressed to S.R. (shacharrichter@gmail.com); Z.Z. (Zeev.Zalevsky@biu.ac.il) or R.J. (razj@bgu.ac.il)

"Beating speckles" via electrically-induced vibrations of Au nanorods embedded in sol-gel

Margarita Ritenberg[1], Edith Beilis[2], Asaf Ilovitsh[3], Zehava Barkai[5], Asaf Shahmoon[3], Shachar Richter[2], Zeev Zalevsky[3,4] & Raz Jelinek[1]

[1]Department of Chemistry and Ilse Katz Institute for Nanoscale Science and Technology, Ben-Gurion University of the Negev, Beer-Sheva 84105, Israel, [2]Center for Nanoscience and Nanotechnology, Tel Aviv University, Tel Aviv 69978, Israel, [3]Faculty of Engineering and Bar-Ilan Institute for Nanotechnology & Advanced Materials, Ramat-Gan 52900, Israel, [4]Friedrich-Alexander Erlangen-Nuremberg University, Erlangen, 91052, Germany, [5]Wolfson Applied Materials Research Center, TAU.

Generation of macroscopic phenomena through manipulating nano-scale properties of materials is among the most fundamental goals of nanotechnology research. We demonstrate cooperative "speckle beats" induced through electric-field modulation of gold (Au) nanorods embedded in a transparent sol-gel host. Specifically, we show that placing the Au nanorod/sol-gel matrix in an alternating current (AC) field gives rise to dramatic modulation of incident light scattered from the material. The speckle light patterns take form of "beats", for which the amplitude and frequency are directly correlated with the voltage and frequency, respectively, of the applied AC field. The data indicate that the speckle beats arise from localized vibrations of the gel-embedded Au nanorods, induced through the interactions between the AC field and the electrostatically-charged nanorods. This phenomenon opens the way for new means of investigating nanoparticles in constrained environments. Applications in electro-optical devices, such as optical modulators, movable lenses, and others are also envisaged.

Among the basic goals in nanotechnology research has been the development of systems in which *macroscopic* phenomena are induced and modulated by the intrinsic properties of *nano-scale* assemblies. The "nanoscale-macroscale" relationship is apparent in many processes and fundamental applications, including piezoelectricity, magnetism, heat conductivity in solids, and also in more specialized phenomena such as quantum coherence. This generic relationship has been particularly encountered in coupled photonic/electronic devices[1–5]. For example, an interesting new concept for realizing nanometric photonic devices on silicon chips focuses on implanting a single gold nanoparticle (Au NP) along the silicon waveguide while externally controlling its photonic tunability[6,7]. In another recent demonstration, realization of optically reconfigurable properties was obtained by illumination of metal nanorod assemblies[8].

In this study, we exploit electro-optic modulation on the nanoscale to form a novel macroscopic photonic modulation concept, based upon encapsulation of Au nanorods in a sol-gel host matrix. Sol-gel materials constitute a unique class of porous and transparent host materials which can readily embed a broad range of chemical and biological guest molecules. In particular, numerous experiments have utilized the *transparency* of sol-gels, making possible the application of diverse spectroscopic and optical techniques for analysis of gel-embedded guest species[9,10]. The porous gel framework also enables co-encapsulation of *solvent* molecules, thus allowing mobility of embedded solute molecules and particles[11].

Nanoparticles (NPs) were incorporated within sol-gel host matrixes and varied reports underscore both the scientific and practical potential of such composite systems[12,13]. *Au NP*/sol-gel architectures, in particular, have been employed in sensing[14,15], controlled release[16,17], and other applications. Utilization of Au NP/sol-gel systems as photonic or electronic conduits, however, has not been reported. Here we report a unique electro-optic phenomenon, directly linked to encapsulation of *Au nanorods* within sol-gel pores. Specifically, we observed light "speckle beats" induced through placing the Au nanorod/sol-gel assembly in an alternating-current (AC) electric field while simultaneously illuminating the sample with a laser beam. The concept we present, besides being a demonstration of interlinked nano-macro phenomena, opens the way to applications in photonic devices, biological imaging, nanostructure characterization, and others.

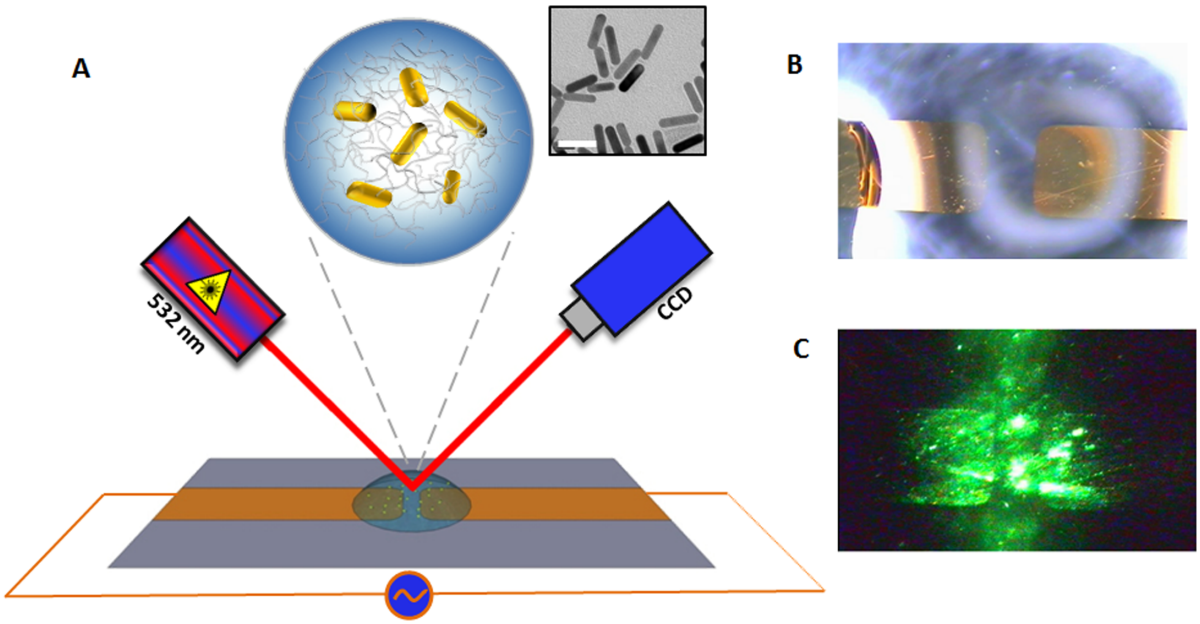

Figure 1 | Experimental setup. (A). Schematic description of the system. Small volume of a sol-gel/Au nanorod assembly was placed in an AC field. The inset shows a transmission electron microscopy (TEM) image of the Au nanorods, scale-bar corresponds to 40 nm. The gel was irradiated simultaneously with application of an AC electric field between the two electrodes and scattered light was recorded by the CCD camera. (B). Photograph of the experimental setup showing a transparent gel placed between two electrodes spaced at 0.5 mm; (C). A speckle pattern recorded by the camera through illumination the sol-gel sample with the green laser (532 nm).

Results

The experimental setup is depicted in Figure 1. Au nanorods, synthesized through conventional protocols[18] were interspersed with the silica precursors of the sol-gel matrix, producing after gelation a transparent sol-gel matrix in which the Au nanorods were embedded within the porous framework. Repeated washing cycles did not remove the nanorods from within the sol-gel matrix, confirming their encapsulation within the gel. Following co-assembly, the Au nanorod/sol-gel construct was placed between two electrodes producing an alternating current (AC) electric field for which both the *voltage* and *frequency* could be externally modulated. Simultaneously with application of the AC field, the nanorod/sol-gel sample was also illuminated by a focused monochromatic laser beam (λ=532 nm) and the scattered light was recorded by a conventional charge-coupled device (CCD) camera.

Figure 1B presents a picture of the Au nanorod/sol-gel electrode setup, showing the sol-gel droplet between the two electrodes. The distance between the electrodes could be engineered to facilitate optimal power input and usage of minute sample volumes (microliter range). Importantly, the experiments were carried out before complete dehydration of the sol-gel, thus motion of the Au nanorods was still enabled within the aqueous solution trapped in the porous sol-gel framework[19].

Application of the AC field gave rise to dramatic modulation of the scattered light. Figure 2 depicts *still images* of a small region within the speckle pattern, extracted from a video recorded using the setup depicted in Figure 1 (the representative video is provided in the Supplementary Information file). Specifically, Figure 2 shows visible "beats" of the monochromatic light scattered from the gel/nanorod assembly (e.g. "speckles"[20]). Note in particular the *intensity modulation* of the speckle pattern shown in Figure 2 indicated by the white rectangle in Figure 2; the beat frequency was precisely correlated with the applied AC.

We carried out a temporal analysis of the recorded images of the back-reflected speckle patterns, such as shown in Figure 2. Specifically, we determined through simple image analysis both the *frequency* of speckle motion, as well as the *amplitude* span of the speckle beats (Figure 3). Significantly, Figure 3 demonstrates that the *amplitude* of the speckle vibration (i.e. difference between minimum and maximum speckle intensities) was dependent upon the AC *voltage amplitude* (Figure 3A), while the *frequency* of the speckle beats was directly correlated to the AC periods (Figure 3B). These relationships establish a direct link between the light modulation and the AC field.

A particularly striking result is the observation of *higher-order harmonics* upon Fourier transformation of the speckle beats (Figure 3C). Importantly, the distinct colors in Figure 3C correspond to different pixels in the pulse area (e.g. analysis of different speckles), demonstrating the universal nature of this phenomenon. The observation of higher harmonics for the beats of the speckle patterns is ascribed to the sinusoidal dependence of nanorod motion within the constrained sol-gel environment, according to the model introduced by Coussot *et al.*[21–23]. Specifically, according to the model:

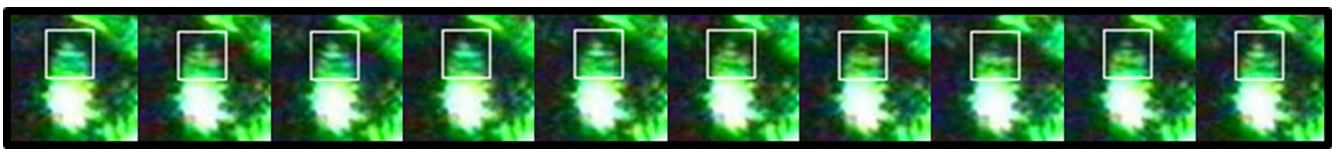

Figure 2 | AC-induced "beats" within a speckle pattern produced upon illumination of the Au nanorod/sol-gel matrix. Images recorded consecutively at voltage of 4 V and at frequency of *4 Hz* of the AC field with simultaneous irradiation with a laser beam (532 nm). The while rectangle highlights the intensity modulation of a specific speckle. The presented images were captured at temporal differences of 25 msec.

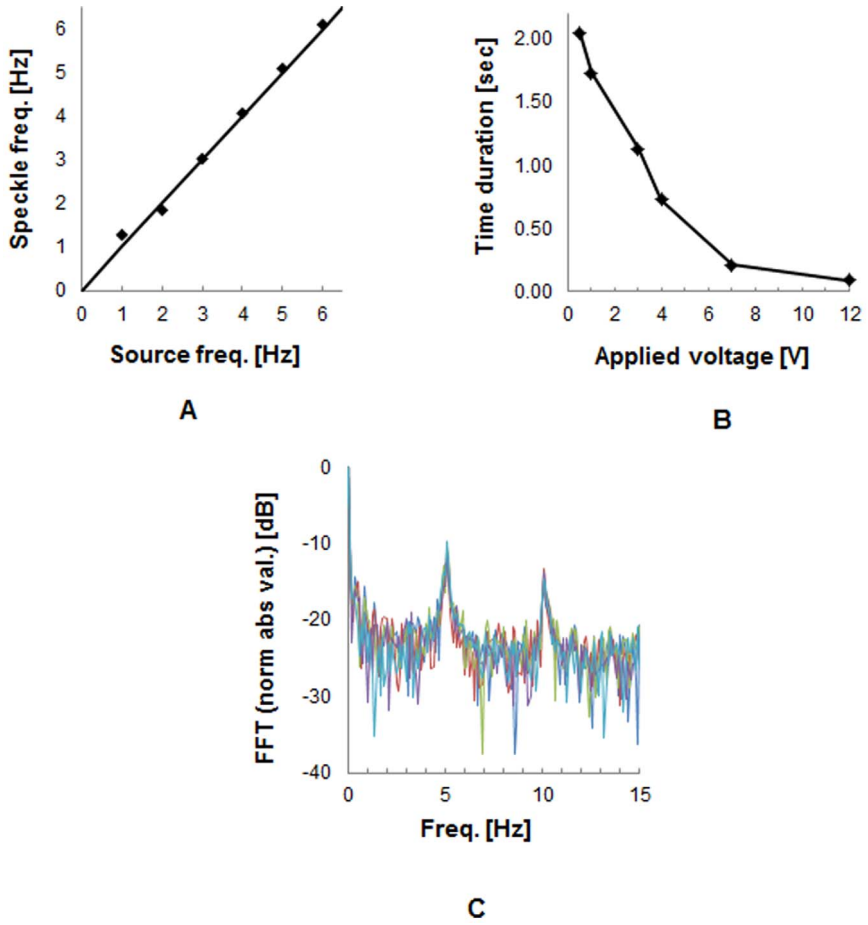

Figure 3 | Correlation between speckle beat properties and electric field parameters. (A). Frequency of speckle flickering versus the frequency of the applied AC electrical field. (B). Periodicity of the flickering occurring in the back reflected speckle patterns as function of the applied voltage of the external field. The measured time duration is proportional to the movement amplitude (the relation constant is the movement velocity). (C). High-order harmonics observed through Fourier transform of the temporal fluctuations of the speckle pattern.

$$\eta = \eta_0(1-\lambda^n) \quad \tau = \eta(\lambda,\dot{\gamma})\dot{\gamma} \tag{1}$$

Where η is the viscosity, τ and $\dot{\gamma}$ are the shear stress and shear rate magnitudes, respectively, depending on the current flocculation state (λ) of the material (e.g. degree of "jamming"). The value of λ is determined by solving the differential equation[24,25]:

$$\frac{d\lambda}{dt} = \frac{1}{\theta} - \alpha\dot{\gamma}\lambda \tag{2}$$

In which θ is the flocculation characteristic time and α is the material parameter. Thus, since the shear stress τ is proportional to the applied force (in our case it is a sinusoidal force induced by the AC field with radial frequency of ω_0), the shear rate $\dot{\gamma}$ as well as the viscosity are depicted as a nonlinear function of the applied sinusoidal force, e.g. includes *higher harmonics* than the radial frequency of the applied sinusoidal force. Mathematically, using the above relations one obtains:

$$\dot{\gamma} = \frac{\tau_0 \sin(\omega_0 t)}{\eta_0(1-\lambda^n)} \tag{3}$$

In which τ_0 is the amplitude of the applied sinusoidal shear stress (proportional to the applied force) and

$$\frac{d\lambda}{dt} = \frac{1}{\theta} - \frac{\alpha\tau_0 \sin(\omega_0 t)}{\eta_0\left(\lambda^{-1}-\lambda^{n-1}\right)} \tag{4}$$

The significance of the analysis introduced by Coussot et al. underscoring the generation of a higher order harmonic peak - is the establishment of a clear quantitative link between the modulated scattered light, the physico-chemical characteristics of the Au nanorod/sol-gel system (e.g. motion of the Au nanorods in the constrained gel environment), and the electric field parameters. Indeed, the theory we present here for the generation of the higher harmonic in the temporal Fourier domain conforms the experimental results in Figure 2C depicting harmonics at frequencies which are multiples of the frequency of the stimulating electrical AC field.

It should be noted that other models have been discussed in the literature, characterizing non linear effects in viscous solutions, particularly focused on *rheology*[26]. The study described in ref. [26], however, analyzes Laponite suspensions which exhibit much lower viscosity than the sol-gel system presented here. This distinction is important, since the model outlined by Coussot et al. is more pertinent to high viscosity systems such as sol-gels. Nevertheless, the intriguing phenomena we report echo the observations that non linear rheology effects are apparent also in lower viscosity liquids, forming the basis to the optical modulation shown in Figures 2 and 3.

Additional experiments were carried out to confirm that the "speckle beats" were directly linked to the motion of Au nanorods within the sol-gel construct induced be the AC field. Specifically, speckle modulation was not observed when an "empty" sol-gel (not containing Au nanorods) was placed in an AC field and illuminated by the laser beam. Similarly, no speckle beats were observed when a direct current (DC) field was applied, nor when Au nanorods in an aqueous solution (not inside a sol-gel) or in a dried film were placed in the AC field (data not shown).

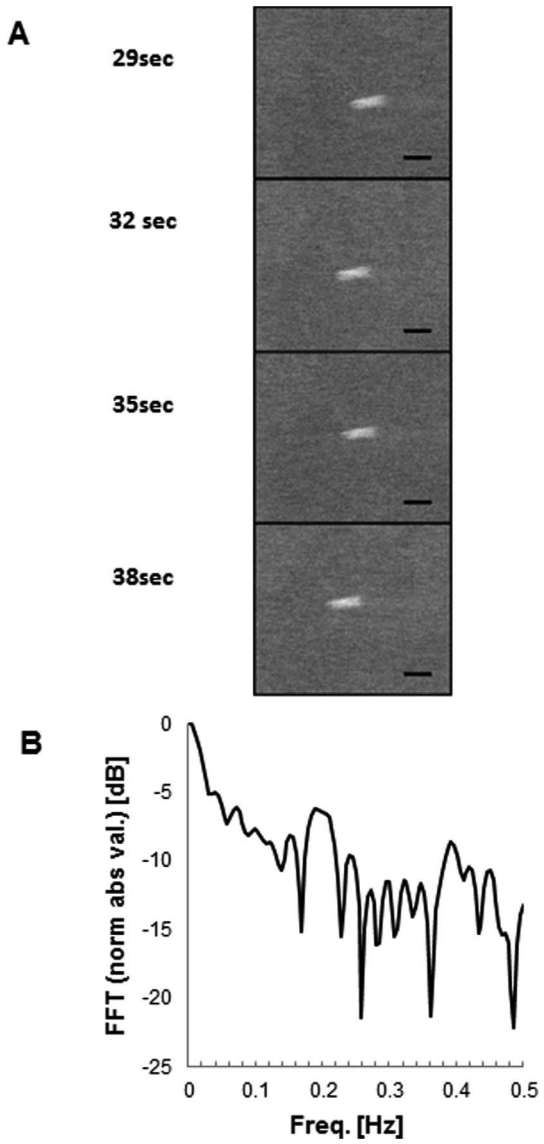

Figure 4 | *In situ* environmental scanning electron microscopy (ESEM). (A). Still images of a sol-gel embedded Au nanorod aggregate placed in an AC field (sinusoidal frequency of 0.2 Hz). The images were extracted in the time-points indicated (the complete video is provided in Figure the Supporting Information). (B). Temporal Fourier transform analysis applied on the spatial region of interest in which nanorod motion was recorded. One may clearly see that the first harmonic appears at 0.2 Hz and the second harmonic at 0.4 Hz.

These observations and the mathematical analysis of the frequency modulation outlined above underscore the correlation between the speckle beating phenomenon and applied AC field. This correlation is ascribed to the electrostatic-charge of the Au nanorod surface - as they are coated by a bilayer of cetyltrimethylammonium bromide (CTAB), which exhibits partial positively-charged headgroups[27]. Consequently, the Au nanorods interact with the externally-applied alternating electrical field. It is important to note that encapsulation of the nanorods within the porous gel framework results in restricted mobility, leading to localized vibrations with amplitude and periodicity that are determined by the AC field. These vibrations are manifested through the spatial-temporal analysis of the back-reflected optical speckle patterns depicted in Figure 3. Indeed, the ensemble of embedded Au nanorods moving in tandem with the applied AC field is the fundamental driving force generating the observed speckle pattern beats.

To further support the above description we carried out in situ environmental scanning electron microscopy (ESEM) experiments designed to visualize the mobility of the gel-embedded Au nanorods while an externally-modulated AC field is applied (Figure 4). Figure 4A depicts still ESEM images of encapsulated Au nanorods, recorded in progressive time-points upon application of the sinusoidal AC field (the complete video file is provided in the Supporting Information). As apparent in Figure 4A (and the video file in the Supporting Information), the frequency of the vibration motion of the nanorods echoes the applied AC frequency.

To quantitatively verify the correlation between the nanorod motion recorded in the ESEM experiment and the applied AC field we carried out a Fourier transformation over the temporal changes visible in the spatial region of interest (Figure 4B), similar to the procedure described above for the optical speckle images (Figure 3C). Importantly, the Fourier transformation yielded a second harmonic frequency peak appearing in the temporal domain, confirming that the AC-induced gold nanorod vibrations recorded in the ESEM experiment indeed correspond to nanorod motion, rather than vibrations of the electron beam, which might be induced by the electric field.

It should be emphasized that the proposed model does not make a direct link between the movements of the gold NPs and the eventual speckle formation due to the ensemble of moving particles. While we have previously established a direct relationship between back-reflected speckle patterns and positions of the reflecting particles[28], the model outlined above is still suggestive and not yet concrete.

Discussion

This work demonstrates a unique phenomenon in which "beats" of optical speckle patterns are introduced through illuminating a Au nanorod/sol-gel assembly placed within an AC electric field. This electrical/optical effect is due to interactions between the applied field and the electrostatically-charged Au nanorods, embedded in the constrained environment of the sol-gel pores. The presented results underscore a unique *macroscopic* physical property (visible vibrations of the speckle pattern) that is directly traced to a *nanoscale* material organization (Au nanorods embedded in sol-gel pores).

The data presented point to direct utilization of the Au NP/sol-gel system as an optical modulator. These applications have attracted significant scientific and technological interest and several reports depicted varied liquid crystal (LC)-based modulator designs[29]. Although LC modulators exhibit significant electro-optic effects, they are significantly smaller than the modulation effect that can be obtained with the Au NPs, since in liquid crystals the electrical field modifies the *refraction index* while in the system depicted here modulation is based upon *NP mobility*. Indeed, we previously showed that transversal movement of only 10 nm is sufficient to obtain modulation with extinction ratio of above 10 dB for axial interaction of about 20 microns[6]. This is not obtainable with LCs.

An important parameter concerns the *concentration* of the Au NPs for which the optical phenomenon arises. As one of the important applications we envision are nano photonic modulators, the minimal concentration would constitute a single nano particle within the cross section of the optical mode multiplied by axial distance of about 20 microns. In case of silicon waveguides this corresponds to a volume of around 200 nm×400 nm×20,000 nm, which is 1.6 (μm^3)[6].

The sol-gel modulator exhibits notable advantages as a possible photonic platform. The sol-gel matrix constitutes a stable, rigid scaffold which allows high repeatability of the modulation effect. The Au nanorod/sol-gel assembly is furthermore simple to manufacture and, as demonstrated above, requires relatively low modulation voltages even if the electrodes are positioned quite far from the waveguide. In addition, although a sol-gel based waveguide would exhibit a lower

refractive index[30], it displays much lower evanescent tails thereby resulting in smaller attenuation from the external electrodes. Furthermore, the Au NP/sol-gel concept might be also used for molecular imaging since via the temporal profile of the mechanical movement of the NPs one could identify the specific type of tissue even without actually imaging it, as e.g. done in conventional imaging approaches.

Methods

Materials. Au(III) chloride trihydrate (≥99.9%), trisodium citrate, sodium borohydride (98%), L-ascorbic acid (99%), tetramethyl orthosilicate, TMOS, (98%), and trizma base were purchased from Sigma-Aldrich. Cetyltrimethylamonium bromide, CTAB, (98%) was received from Alfa Aesar (USA). Silver nitrate was purchased from Metalor Technologies Ltd (UK). Hydrochloric acid (HCl) was purchased from Gadot Biochemical Industries Ltd (Israel). All chemicals were used as received. Water used in all experiments was de-ionized up to 18.2 MΩ cm resistivity (Barnstead/Thermolyne Corporation, Dubuque, IA).

Au nanorod synthesis. Positively-charged Au nanorods were synthesized according to the two-step seed-mediated growth method described by Nikoobakht and El-Sayed. First, *seed solution* was prepared by mixing 5 mL of 0.2 M CTAB solution with 5.0 mL of 0.0005 M chlorauric acid ($HAuCl_4$). To the stirred solution, 0.60 mL of ice-cold 0.010 M sodium borohydride ($NaBH_4$) was added, resulted in the formation of a brownish yellow solution. Vigorous stirring of the seed solution was continued for several minutes. Following stirring, the solution was kept at room temperature. *Growth solution* was prepared by mixing 5 mL of 0.2 M CTAB solution with 0.2 mL of 0.0040 M silver nitrate ($AgNO_3$) solution at room temperature. 5.0 mL of 0.0010 M $HAuCl_4$ was subsequently added, and after gentle mixing 70 μL of 0.0788 M ascorbic acid was added. As a result the growth solution changed its color from dark yellow to colorless. The final step was the addition of 12 μL of the seed solution to the growth solution at 30°C. The color of the solution gradually changed within 50 min. In order to separate nanorods from excess CTAB, the solution was centrifuged at 13000 rpm for 10 min. The supernatant was removed and the nanorods were re-suspended in appropriate volume of double de-ionized water (DDW). The washing process was repeated 3 times.

Au nanorod/sol-gel preparation. The sol-gel precursor solution was prepared by mixing 4.41 ml TMOS, 2.16 ml DDW, and 0.06 ml HCl (0.62 M) at 4°C for 1 h. The resulted prehydrolyzed TMOS sol was kept at −20°C before use. For preparing the composite Au nanorod/sol-gel sample, equal amounts of the prehydrolyzed sol and Au nanorod solution were mixed together. Subsequently, Tris buffer (50 mM, pH=8) was added to the nanorods/sol solution in a 1 : 1 volume ratio at room temperature. Gelation occurred within minutes after buffer addition, accordingly all measurements were carried out immediately after sample preparation.

Transmission electron microscopy (TEM). 10 μL of the nanorod solution was applied to 400-mesh copper formvar/carbon grid (Electron Microscope Sciences, Hatfield, PA, USA), and then allowed to dry in air. Afterwards, Au nanorod samples were characterized using 200 kV JEOL JEM-2100F Transmission electron microscope (USA).

Electro-optical experimental setup. Arrays of gold electrodes on silicon or glass surfaces (electrode spacing 500 μm) were fabricated using the appropriate shadow masks and gold evaporation, followed by welding low-noise electrical cables to the electrodes. The light modulation experiment was videoed under microscope while a green laser at wavelength of 532 nm and power of 50 mW illuminated the sample.

In-situ environmental scanning electron microscopy (ESEM). Experiments were carried out on an FEI Quanta 200 field emission gun (FEG) environmental SEM (ESEM). The samples in the ESEM were mounted on a Peltier cooling stage, which was externally water-cooled. This allowed imaging the samples at wet mode (initial conditions typically were 2°C and 5.3 torr), while applying external AC electric fields on the sample electrodes via chamber feed-through leads connected to an external voltage supplier. Video recording was done in a frequency of 10 Hz, which was greater than the electric field frequency (0.2 Hz) in order to avoid coupling between the ESEM scanning and the external electric field.

Data analysis. Temporal light beat analysis was carried out through recording the speckle pattern reflected from the Au nanorod/sol gel, and then choosing the spatial region of interest. The temporal information (flickering of the speckle) was Fourier transformed. In the spectrum we analyzed both the *temporal frequency* at which the flickering occurred as well as the *amplitude* at which the speckle patterns were flickering.

1. Samara-Rubio, D. *et al.* Customized drive electronics to extend silicon optical modulators to 4 Gb/s. *J. Lightwave Technol.* **23**, 4305–4314 (2005).
2. Yabu, T., Geshiro, M., Kitamura, T., Nishida, K. & Sawa, S. All-optical logic gates containing a two-mode nonlinear waveguide. *IEEE J. Quant. Electron.* **38**, 37–46 (2002).
3. Scheuer, J., Paloczi, G. T. & Yariv, A. All optically tunable wavelength-selective reflector consisting of coupled polymeric microring resonators. *Appl. Phys. Lett.* **87**, 1–3 (2005).
4. Yanik, M. F., Fan, S., Soljačić, M. & Joannopoulos, J. D. All-optical transistor action with bistable switching in a photonic crystal cross-waveguide geometry. *Opt. Lett.* **28**, 2506–2508 (2003).
5. Kato, M., Kumtornkittikul, C. & Nakano, Y. Wavelength conversion using polarization dependence of photo-induced phase shift in an InGaAsP MQW-EA modulator. *ThDD3* 595–596 (2002).
6. Limon, O. *et al.* Fabrication of electro optical nano modulator on silicon chip. *Microelectron. Eng.* **86**, 1099–1102 (2009).
7. Shahmoon, A. *et al.* All-optical nano modulator, sensor, wavelength converter, logic gate, and flip flop based on a manipulated gold nanoparticle. *J. Nanophotonics* **4**, 1–10 (2010).
8. Meiri, A., Shahmoon, A., Businaro, L. & Zalevsky, Z. Optically reconfigurable structures based on surface enhanced Raman scattering in nanorods. *Microelectron. Eng.* **111**, 251–255 (2013).
9. Frenkel-Mullerad, H. & Avnir, D. Sol-gel materials as efficient enzyme protectors: preserving the activity of phosphatases under extreme ph conditions. *J. Am. Chem. Soc.* **127**, 8077–8081 (2005).
10. Dunn, B. & Zink, J. Optical properties of sol-gel glasses doped with organic molecules. *J. Mater. Chem.* **1**, 903–913 (1991).
11. Wheeler, K. E. *et al.* Electrostatic influence on rotational mobilities of sol-gel-encapsulated solutes by NMR and EPR spectroscopies. *J. Am. Chem. Soc.* **126**, 13459–13463 (2004).
12. Schmidt, H., Jonschker, G., Goedicke, S. & Mennig, M. The sol-gel process as a basic technology for nanoparticle-dispersed inorganic-organic composites. *J. Sol-Gel Sci. Technol.* **19**, 39–51 (2000).
13. Vivero-Escoto, J. L. & Huang, Y.-T. Inorganic-organic hybrid nanomaterials for therapeutic and diagnostic imaging applications. *Int. J. Mol. Sci.* **12**, 3888–3927 (2011).
14. Jia, J. *et al.* A method to construct a third-generation horseradish peroxidase biosensor: self-assembling gold nanoparticles to three-dimensional sol−gel network. *Anal. Chem.* **74**, 2217–2223 (2002).
15. Jena, B. K. & Raj, C. R. Electrochemical biosensor based on integrated assembly of dehydrogenase enzymes and gold nanoparticles. *Anal. Chem.* **78**, 6332–6339 (2006).
16. Torney, F., Trewyn, B. G., Lin, V. S.-Y. & Wang, K. Mesoporous silica nanoparticles deliver DNA and chemicals into plants. *Nat. Nanotechnol.* **2**, 295–300 (2007).
17. Vivero-Escoto, J. L., Slowing, I. I., Wu, C.-W. & Lin, V. S.-Y. Photoinduced intracellular controlled release drug delivery in human cells by gold-capped mesoporous silica nanosphere. *J. Am. Chem. Soc.* **131**, 3462–3463 (2009).
18. Nikoobakht, B. & El-Sayed, M. A. Preparation and growth mechanism of gold nanorods (NRs) using seed-mediated growth method. *Chem. Mater.* **15**, 1957–1962 (2003).
19. Dunn, B. & Zink, J. I. Probes of pore environment and molecule - matrix interactions in sol - gel materials. *Chem. Mater.* **9**, 2280–2291 (1997).
20. Goodman, J. W. Some fundamental properties of speckle. *J. Opt. Soc. Am.* **66**, 1145–1150 (1976).
21. Barnes, H. A. Thixotropy- a review. *J. Non-Newtonian Fluid Mech.* **70**, 1–33 (1997).
22. Coussot, P., Nguyen, Q., Huynh, H. & Bonn, D. Avalanche behavior in yield stress fluids. *Phys. Rev. Lett.* **88**, 1–4 (2002).
23. Roussel, N. A thixotropy model for fresh fluid concretes: Theory, validation and applications. *Cem. Concr. Res.* **36**, 1797–1806 (2006).
24. Lifshitz, R., Arie, A. & Bahabad, A. Photonic quasicrystals for nonlinear optical frequency conversion. *Phys. Rev. Lett.* **95**, 1–4 (2005).
25. Sharping, J. E., Fiorentino, M., Kumar, P. & Windeler, R. S. All-optical switching based on cross-phase modulation in microstructure fiber. *IEEE Photon. Technol. Lett.* **14**, 77–79 (2002).
26. Abou, B., Bonn, D. & Meunier, J. Nonlinear rheology of Laponite suspensions under an external drive. *J. Rheol.* **47**, 979–988 (2003).
27. Nikoobakht, B. & El-Sayed, M. A. Evidence for bilayer assembly of cationic surfactants on the surface of gold nanorods. *Langmuir* **17**, 6368–6374 (2001).
28. Beiderman, Y. *et al.* A microscope configuration for nanometer 3-D movement monitoring accuracy. *Micron* **42**, 366–375 (2011).
29. Beeckman, J., Neyts, K. & Vanbrabant, P. J. M. Liquid-crystal photonic applications. *Opt. Eng.* **50**, 081202(1–17) (2011).
30. Soref, R. & Bennett, B. Electrooptical effects in silicon. *IEEE J. Quant. Electron.* **23**, 123–129 (1987).

Acknowledgments

Financial support by the Ministry of Science, Tashtiot Fund is acknowledged.

Author contributions

M.R., E.B., A.I., A.S. carried out the experiments; Z.B. contributed experimental planning and carried out the SEM experiments; S.R., Z.Z. and R.J. planned the experiments and wrote the manuscript. All authors reviewed the manuscript.

Additional information

Supplementary information accompanies this paper at http://www.nature.com/scientificreports

Competing financial interests: The authors declare no competing financial interests.

How to cite this article: Ritenberg, M. *et al.* "Beating speckles" via electrically-induced vibrations of Au nanorods embedded in sol-gel. *Sci. Rep.* **4**, 3666; DOI:10.1038/srep03666 (2014).